DOI:10.16555/j.1006-8775.2015.02.004

Article ID: 1006-8775(2015) 02-0131-12

COMPARISONS OF CIRCULATION ANOMALIES BETWEEN THE DAILY PRECIPITATION EXTREME AND NON–EXTREME EVENTS IN THE MIDDLE AND LOWER REACHES OF YANGTZE RIVER IN BOREAL SUMMER

HAN Jie (韩 洁)[1,2], GUAN Zhao-yong (管兆勇)[1], LI Ming-gang (李明刚)[1]
(1. Key Laboratory of the Ministry of Education for Meteorological Disaster in Nanjing University of Information Science & Technology, Nanjing 210044 China; 2. Baoji Meteorological Bureau, Baoji, Shaanxi 721006 China)

Abstract: Based on the NCEP/NCAR reanalysis dataset and in situ meteorological observations of daily precipitation in boreal summer from 1979 to 2008, the features of circulation anomalies have been investigated using the composite analysis for the extreme events and non-extreme events of regional mean daily rainfall (RMDR) occurring over the mid- and lower- Yangtze valley (MLYV). The extreme RMDR (ERMDR) events are the events at and above the percentile 99 in the rearranged time-series of the RMDR with ascending order of rainfall amount. The non-extreme RMDR events are those at the percentiles 90-85 and 80-75 separately. Our results suggest that the threshold value is 25 mm/day for the ERMDR at percentile 99. Precipitation at all the percentiles is found to occur more frequently in the Meiyu rainfall season in MLYV, and the ERMDR events have occurred with higher frequency since the 1990s. For the percentiles-associated events, the MLYV is under the control of an anomalous cyclonic circulation in the mid- and lower- troposphere with vastly different anomalous circulation at higher levels. However, at both low and high levels, the ERMDR events-related anomalous circulation is stronger compared to that linked to the non-ERMDR events. The dominant sources of water vapor differ between the ERMDR and non-ERMDR events. During the ERMDR events plentiful water vapor is transported from the Bay of Bengal into the MLYV directly by divergence while there is distinctly increased water vapor from the South China Sea (SCS) in non-RMERMDR episodes. The diabatic heating rates $< Q_1 >$, $< Q_2 >$ and $< Q_1 > - < Q_2 >$ have their anomalous patterns and are consistent with each other for these percentiles but their strength decreases markedly with the drop of rainfall intensity. For the precipitation at percentiles 99 and 90-85, the sea surface temperature anomalies (SSTA) in the Pacific distribute positively (negatively) in the south (north), and are stronger when the ERMDR emerges, with little or no SSTA as the events at percentile 80-75 occur. Besides, these results suggest that the genesis of the ERMDR event is directly related to intense local circulation anomalies and the circulation anomalies over the Pacific and SCS in tropical to mid-latitudes, and probably linked with the Pacific SSTA closely while the non-ERMDR events are mainly associated with the anomalous circulation on a local basis. The findings here help understand and predict the happening of ERMDR events over the MLYV.

Key words: extreme regional mean daily rainfall; non-extreme daily rainfall; circulation features; mid- and lower-Yangtze valley; sea surface temperature anomaly
CLC number: P426.6 **Document code:** A

1 INTRODUCTION

The mid- and lower- Yangtze valley (MLYV) is a region developed industrially and populated densely, where floods/droughts occur frequently. It is in a subtropical monsoon climate, with 50% of total yearly rainfall falling in summer. Early in summer when the Meiyu/Baiu precipitating period is long, disasters are extremely possible. In July-August the region is under the control of a subtropical high, leading to hot weather, which, if long enough, would cause heavy drought (Ma et al.[1]). Therefore, summer rainfall anomalies, particularly extreme regional mean daily rainfall (ERMDR) episodes and droughts, have drawn widespread concern from the general public and meteorologists.

Many studies have been published concerning the MLYV rainfall intensity and causes. The MLYV yearly total rainfall exhibits a mildly increasing trend, owing mainly to the increasing trends of summer and winter precipitation (Zhao et al.[2]; Bai and Liu[3]). In summer, the Meiyu rainfall strength/duration, total amount, the speed of eastward propagating Somali jet with the difference in the longitude wherefrom it turns northward around the South China Sea (SCS) (Guan and Lin[4]), and the variation in the position and intensity of a subtropical high in the western Pacific (Wand et al.[5]) are

Received 2014-05-21; **Revised** 2015-02-26; **Accepted** 2014-04-15
Foundation item: National Natural Science Foundation of China (41330425); National Key Technology R&D Program (2007BAC29B02); "Qinglan" Project of Jiangsu Province for Cultivating Research Teams
Biography: HAN Jie, primarily undertaking research on monsoon dynamics.
Corresponding author: GUAN Zhao-yong, E-mail: guanzy@nuist.edu.cn

all responsible for the precipitation features in summer over the MLYV. The floods often emerge in the developing and decaying stages of an El Niño episode. During its development the subtropical high is more westward than normal and the monsoon systems over the North-Western Pacific (NWP), Eastern Asia and Indonesia display a strengthening trend, with the rainbelt staying unchanged over the Yangtze-Huaihe Rivers basin, Korean Peninsula and Japan, where strong rainfall happens (Li et al.[6]; Tao et al.[7]; Zhang et al.[8]; Wang et al.[9]; Guan and Li[10]). The Indian Ocean Dipole (IOD) is well correlated to the June-August precipitation over China (Saji and Yamagata[11]). In a La Niña (El Niño) year with a negative (positive) IOD occurring, the precipitation increases (decreases) over the MLYV (Yang et al.[12]). A composite analysis was conducted of intraseasonal oscillation (ISO) period, intensity and phase in typical years of floods and droughts, which indicated that the precipitating ISO period is longer in the wet than in the dry year over the MLYV (dominantly 30-60 as against 10-30 day periods) (Wang and Ding[13]). Besides, the severe floods in the MLYV bear a close linkage to an Asian extratropical blocking situation (Tao et al.[14]), the tropical winter monsoon over East Asia (Zhi et al.[15]), the thermal forcing of the Tibetan Plateau (Zhang and Tao[16]) and the preceding spring annular mode appearing in the Southern Hemisphere (Wu et al.[17]). These scientists, however, did not make intensive study on extreme MLYV rainfall events.

In the analysis of precipitation, more attention was directed towards recent strong rainfall events occurring in 1991, 1998 and 2003. In 1991, for example, the coupling of lower-level high-frequency (15-35 days) anomalous anticyclone components with a filtering-treated upper-air dipole-type cyclone causes the Southern-Asian high to extend eastward (Mao and Wu[18]), and mid- (low-latitude) positive (negative) sea surface temperature anomalies (SSTAs) (Xu[19]) to be in the eastern Atlantic, all of which are important factors responsible for severe floods in the Yangtze-Huaihe Rivers region. In 1998 with the background of El Niño two episodes of atmospheric vigorous low-frequency oscillation came from the southern SCS, transporting large quantities of moist air and unstable energy into the Yangtze-Huaihe Rivers valleys and the adjustment of a stationary wavetrain in the southern westerlies provided a necessary background for catastrophic flooding in the MLYV[14]. In their research into upper-level baroclinic wave activities during the Meiyu rainfall period in 1998 and 2003 over the MLYV, Mei and Guan's studies (Mei and Guan[20-21]) have shown the baroclinic wave packet activity to be probably a necessary condition for the happening and developing of strong rainfall there. In 2003 anomalies of apparent SCS heat source $<Q_1>$ and apparent water vapor sink $<Q_2>$ are likely to be one of the causes for the southward than normal position of the subtropical high (Wang et al.[22]), which carries abundance of water vapor into the MLYV, to which rich amount of it is also transported by means of the Indian and SCS monsoonal circulations (Zhou et al.[23]). These conditions are in favor of the occurrence and maintenance of heavy rain, producing severe floods over the Yangtze-Huaihe Rivers basin as a whole.

In recent years multiple studies have been performed of extreme precipitation (Kunkel et al.[24]; Yamamoto and Sakurai[25]), which indicated that in regions with increased total rainfall, it is most likely that the number of extreme precipitation events is increased at even higher proportion. As shown in Qian and Lin[26], areas of pronouncedly increasing trends in extreme rainfall episodes are in the MLYV. However, the happening patterns and causes of these episodes, especially those occurring over a whole-extent valley, need to be explored. Accordingly, following the related definition, these extreme episodes covering the MLYV are divided into 99 percentiles, with percentile 99 for extreme events, percentiles 90-85 and 80-75 for non-ERMDR events taken in study, followed by composite analysis of circulation features related to the three categories of rainfall intensity in order to find out these percentile-based rainfall-event features and seek for clues to predicting strength-differing episodes in the MLYV.

2 DATA AND METHODS

The used data consist of CMA National Meteorological Information Center - provided summer daily rainfall from 743 stations of China, and NCEP/NCAR daily reanalysis (Kalnay et al.[27]) that include the global monthly-mean and day-to-day 17-level geopotential heights and winds at the resolution of 2.5°×2.5° latitude/longitude with June, July and August (JJA) for the summer in 1979-2008. The anomalies or departures of a physical quantity refers to its difference from the multi-year mean climatology, which means that data of a variable are subject to the averaging over 92 days in summer and re-averaged across the 30 years.

The MLYV covers an extensive region north of the Nanling Mountains (25°N), south of the Qinling Mountains and Huaihe River (34°N) and east of the Wushang Mountains (110°E). The rainfall data were taken from 84 stations within Hunan, Hubei, Zhejiang, Jiangxi, Jiangsu and Shanghai, where the stations are distributed more evenly and densely (Fig.2a) compared to stations in other parts of the country. Arithmetic mean was utilized for the regional mean instead of the area averaging furnished by Jones et al.[28] and the interpolation errors are minimized as much as possible.

To explore the relationship of rainfall to heating fields, $<Q_1>$ (apparent heat source) and $<Q_2>$ (apparent water vapor sink) are investigated using the expressions below (Luo and Yanai[29]), i.e.,

$$Q_1=c_p\left(\frac{\partial T}{\partial t}+V \quad \nabla T+\left(\frac{p}{p_0}\right)^k\omega\frac{\partial\theta}{\partial p}\right), \tag{1}$$

$$Q_2=-L(\frac{\partial q}{\partial t}+V\quad\nabla q+\omega\frac{\partial q}{\partial p}). \tag{2}$$

Both the above equations include three terms for local change, horizontal advection and vertical transport, respectively and vertical integration is made of each of the expressions, leading to

$$<Q_1>=\frac{1}{g}\int_{p_T}^{p_S} Q_1 dp=(LP_r+LC-LE)+Q_S+<Q_R>, \tag{3}$$

$$<Q_2>=\frac{1}{g}\int_{p_T}^{p_S} Q_2 dp=(LP_r+LC-LE)-LE_S, \tag{4}$$

$$<Q_1>-<Q_2>=<Q_R>+(Q_S+LE_S). \tag{5}$$

where L denotes condensation latent heat, P_r the rainfall, Q_s the transport of surface sensible heat, E the evaporation rate of air-column cloud droplets, C the rate of condensation per unit mass of air, Es the transport of surface latent heat, $<Q_R>$ the vertical integration of radiative heating (cooling), Ps the surface pressure and PT the pressure at top level (300 hPa here).

To better understand the features of each of the three categories of daily heavy rainfall, the characteristics of the extreme rainfall event are studied and compared with those of the other two types to obtain their differences and linkage.

3 DEFINITION OF ERMDR OVER MLYV AND ITS VARIATIONS

Heavy rain, if occurring only at a single or a limited number of stations, exerts less strong impacts, and when it happens in many places of a whole valley, large-scale floods are possible. Therefore, the daily precipitating amounts will be averaged on a regional basis to determine the number of days for these percentiles throughout the valley.

The total number of days is 2 760 for June to August in 1979-2008, whose daily rainfall values from 84 stations selected (dots given in Fig.2a) and daily rainfall data are regionally averaged, followed by removal of the days at daily rainfall <1 mm, and data of the remaining days are arranged in an increasing order, with the values at percentile 99 taken as a threshold (25.0 mm/day). The days in excess of the thresholds are defined as those of ERMDR. Following the ERMDR definition, 19 episodes at percentile 99 are designated as the whole-valley ERMDR events (not referring to some stations), with the rainfall put into category A, and rainfall of 108/111 events are denoted at percentiles 90-85 and 80-75, with precipitation put in categories C/E, respectively (Table 1).

Table 1. MLYV rainfall thresholds, percentile and category.

Category	Rainfall thresholds (mm/d)	Percentiles (P.)
A	$P_A>25.0$	100≥ P.>99
B	$25.0\geq P_B\geq 15.0$	99≥ P.≥ 90
C	$15.0>P_C>12.8$	90>P.>85
D	$12.8\geq P_D\geq 10.9$	85≥ P.≥ 80
E	$10.9>P_E>9.3$	80>P.>75
F	$9.3\geq P_F>0.0$	75≥ P.>0.0

Figure 1a depicts the number of events during each ten-day period of JJA at the three percentiles including A, C, and E, indicating that the maxima of extreme daily rainfall (ERMDR) occur over the MLYV predominantly in June and early July, in certain relation to the Meiyu precipitating stage. Besides, such events reduce greatly in number after mid-July, during which time the valley is under the effect of prime hot summer. In addition, category C rainfall episodes are nearly equal to those of ERMDR, differing largely in the decreased number in mid-August. However, the number of category E events is different to some extent, just with a peak from mid-June to early July and another one during the middle to last ten-day of August. Accordingly, the valley-extent ERMDR episodes bear a close association with the Meiyu rainy-season rainfall. Categories C and E events are possible on a ten-day basis, particularly in the Meiyu/Baiu season.

ERMDR events are marked by significant interannual variations (Fig.1b). The ERMDR events happened three times in 1994 and they are the highest among these years in sharp contrast to none in 2004-2008. The two categories of rainfall share the increase in daily precipitation events subsequent to the 1990s, a conclusion that is in agreement with that of Su et al.[30].

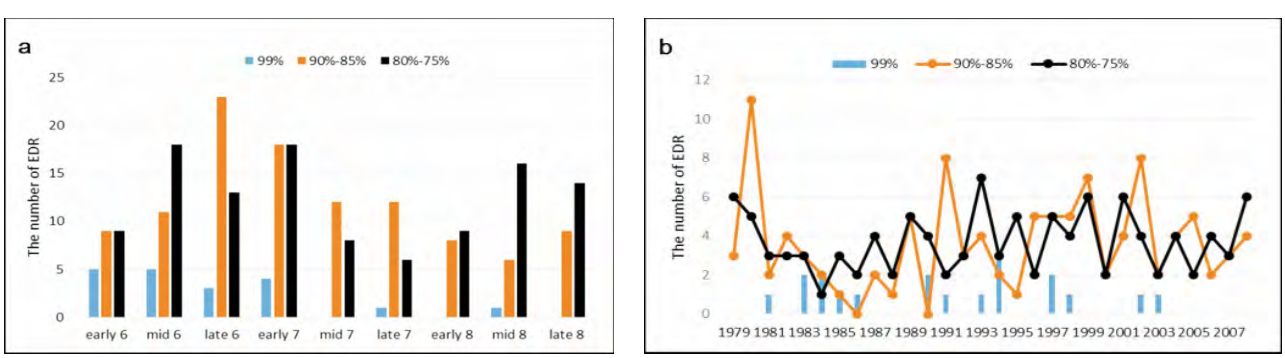

Figure 1. Ten-day-to-ten-day (a) and year-to-year variability (b) in the number of rainfall events at percentiles 99, 90-85 and 80-75 in the summers of 1979-2008 over the MLYV. The ordinate denotes the number of extreme daily rainfall episodes in (b).

4 CHARACTERISTICS OF EXTREME RAINFALL EVENTS

4.1 *Distribution of rainfall values of ERMDR episodes over the MLYV*

To determine the ERMDR-related rainfall, we make a plot to show the mean values over the 19 events and their differences from the 1979-2008 summer climatology, with the finding that the strongest precipitation events are in the juncture of the provinces of Jiangxi, Zhejiang and Anhui, with the maximum even in excess of 60 mm/d, and another higher-value center of not less than 35 mm/d resides in northwest Hunan (Fig. 2a). The rainfall intensity right on both sides along the mid- and lower- Yangtze and in the Jiangnan region is markedly more than in the counterpart north of the Yangtze. The pattern of differences (Fig.2b) is almost the same as in Fig.2a, with the highest and secondary highest values emerging in the 3-province juncture and the northwestern Hunan, respectively.

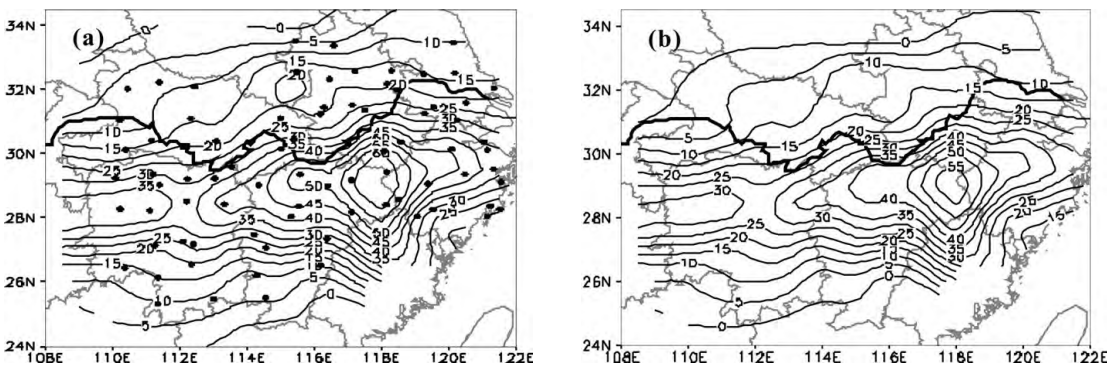

Figure 2. Means over the ERMDR episodes (a) and their differences from the 1979-2008 summertime climatology (b) for the MLYV. Units are in mm/d. The dots thereof denote the selected 84 stations for study in (a). The bold solid line designates the Yangtze River.

4.2 *Anomalies of ERMDR-related circulations*

The happening of ERMDR events in the MLYV is closely linked to the anomalies of local circulations (Tao and Xu [31]; Chen and Qian [32]). By deducting the summer averaged stream field from the equivalent of each of the 19 ERMDR events, followed by the differences composing and comparing to the original field, we derive the anomalies of the non-divergent and divergent winds and vertical circulation (Fig.3). In the middle and lower troposphere (Fig.3a, b) the studied MLYV is under the influence of cyclonic departure circulation, in comparison to an anomalous anticyclonic circulation at lower latitudes that dominates the South China Sea and the western North Pacific. At upper levels (Fig.3c) a vigorous cyclonic departure circulation is at higher latitudes and an anticyclonic counterpart is at low latitudes, whose location is distinctly more westward of normal location, exposing the MLYV to the control of anomalously zonal airflows. In mid- and lower- troposphere over the MLYV there exists pronounced convergence of air from the western Pacific. In higher troposphere the anomalous cyclonic circulation north of the Yangtze and the anomalous anticyclonic circulation to the south benefit air divergence, favoring the maintenance of lower-level convergence. This baroclinic structure of circulations from lower to high levels is highly beneficial to the genesis of ERMDR events.

Anomalies of vertical circulation exhibit a structure favorable for ERMDR episodes. Fig.3d shows a section of anomalies of meridional circulation along 110°-125°

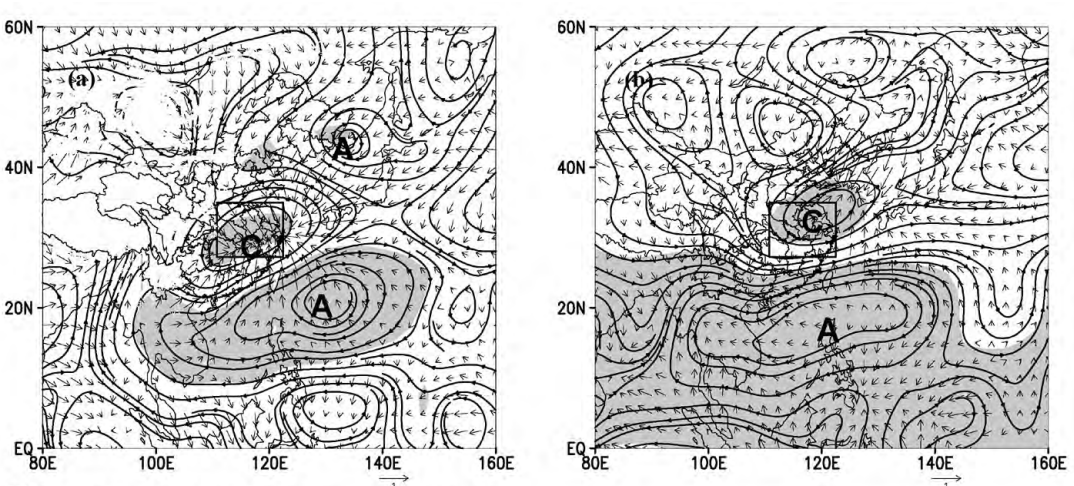

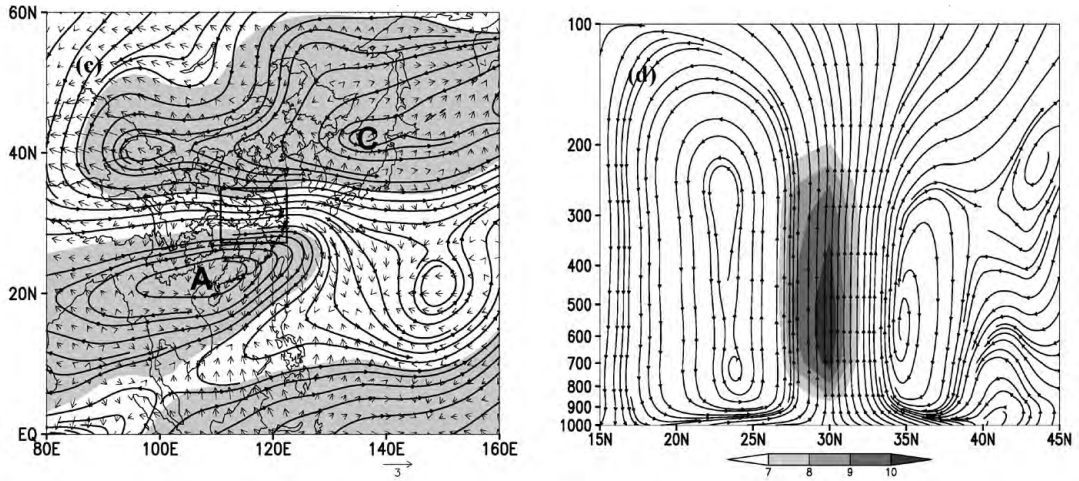

Figure 3. Anomalies of ERMDR-related rotational wind flow (streamlines), and superimposed divergent winds (m/s, arrows) at 850 (a), 500 (b), 200 hPa (c), and a 110° to 125°E cross section of departures of meridional circulation (d), with ω multiplied by a factor of 100. The shading of Fig.3a, b, c denotes the values significant at not less than 95% level of confidence using a *t*-test.

E, and a zone of abnormal strong rising air (shaded) around 30°N, with the departures larger than or equal to 10 Pa/s at the center of vertical velocity. Such large-scale vertical motion provides water vapor condensation with dynamic condition.

In summer, the MLYV is influenced by eastern-Asian and southern-Asian summer monsoons, and the water vapor reaching the valley comes mainly from the Bay of Bengal, SCS and western Pacific (Murakami [33]; Ding[34]). We see that the pattern of stream functions of anomalies of the water vapor fluxes integrated from surface to 300 hPa and that of the divergent components (Fig.4) look roughly similar to those of anomalies of circulation at 850 hPa, such that the water vapor moves from the Bay of Bengal and SCS by dint of the air in the outer-region of the anomalous anticyclonic circulation into the MLYV, where extremely strong convergence occurs, with a convergent band directed in NE-SW, a condition that provides the ERMDR with large amounts of water vapor.

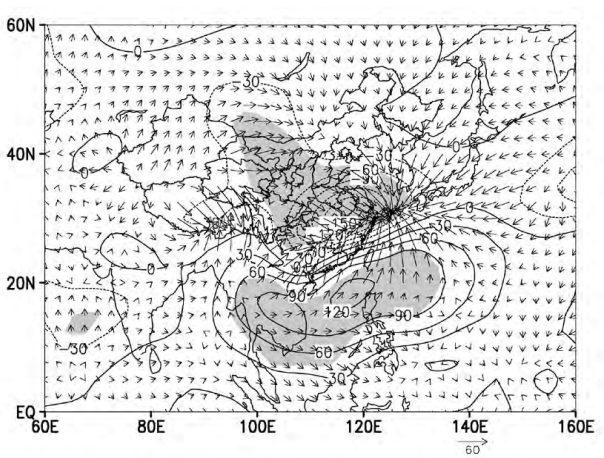

Figure 4. Streamfunctions (106 kg/s) of all ERMDRs composite departures of the vertical extent integrated water vapor flux with the divergent components given in unit of kg/ (m s). The shading denotes values statistically significant at not less than 95% level of confidence using a *t*-test.

4.3 *Anomalies of ERMDR-related heating*

As in the study of Luo and Yanai[29], we present the differences between the composite heating and 1979-2008 mean climatology (Fig.5). Evidently, the patterns of anomalies of apparent heat source ($<Q_1>$, Fig. 5a) and apparent water vapor sink ($<Q_2>$, Fig.5b) are roughly consistent, with their maxima emerging in the MLYV and their magnitudes comparable. As shown in Ding [34], when intense rainfall takes place, only a small amount of surface sensible heat and evaporation occurs, strong apparent water vapor sink causes heavy rainfall that releases large quantities of condensation heat, thereby producing diabatic heating in the air, which gives rise to the reduction of surface pressure, playing a positive-feedback role in temperature rise. Negative departure centers of $<Q_1>$ and $<Q_2>$ emerge in the SCS and western North Pacific (Fig.5a, b), in relation to the area under the impact of a subtropical high and subsidence within it[22].

To further determine the role of diabatic heating, the anomalies of $<Q_1>$ - $<Q_2>$ are given in Fig.5c. If the differences are very small, then water vapor condensation is predominant; if the differences are of positive (negative) anomalies, then radiation heating (cooling) and transport of surface sensible/latent will be strengthened (weakened) in addition to latent heating. Additionally, Fig.5c shows that the positive anomalies of $<Q_1>$ - $<Q_2>$ are in a zone that is more northern from the MLYV, suggesting that radiation and the transport of surface sensitive/latent are anomalously increased there, maybe associated with the fact that the principal rainfall zones have moved to the Jiangnan region. Negative departures of the diabatic heating are found in the southeastern part and seaboard of the MLYV, a situation un-

favorable for the genesis of air-column heating and rising motion. Negative anomalies are also found in 120° -140°E around 15°N, implying that there are decreased sea surface thermal fluxes and intensified radiation cooling, conditions that benefit the weakening of air rising and anomalies of latent heat release as well as the divergence at lower levels. Following Gill's theory of atmospheric response to thermal forcing (Gong and He[35]), such negative diabatic heating favors the genesis of an anticyclonic circulation northwest of this zone, further exciting a wave train traveling eastward and then northward, consequently furnishing ERMDR occurrence with a large-scale disturbance background.

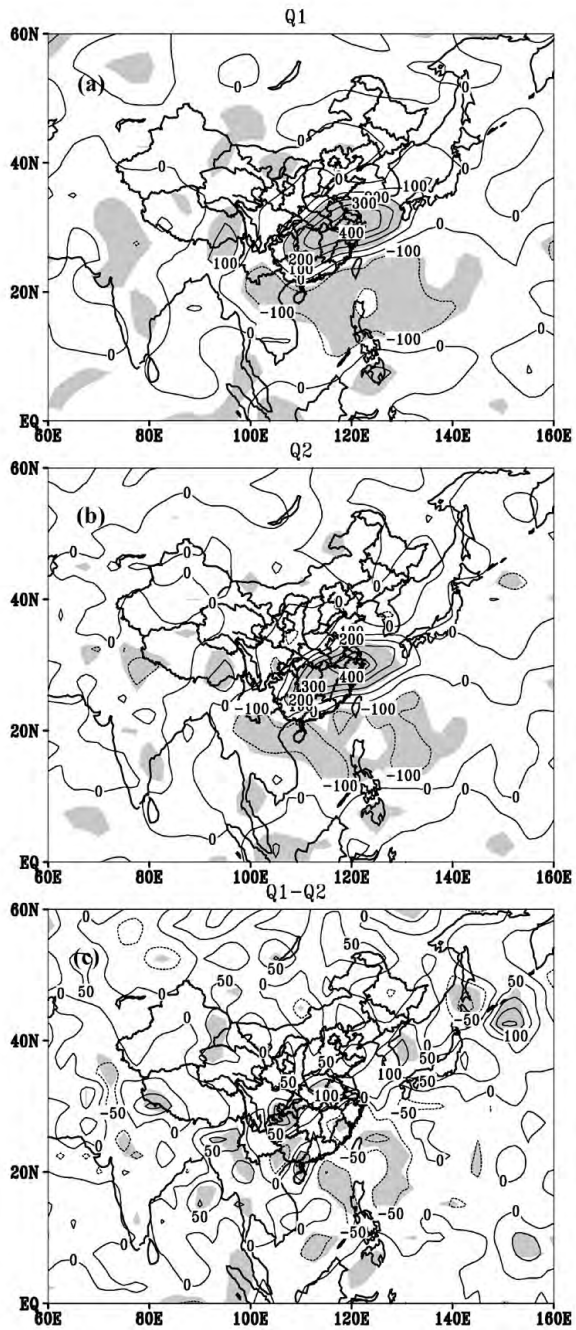

Figure 5. The 19 ERMDR events-based composite vertically integrated apparent heat source (<Q_1>, a), apparent water vapor sink (<Q_2>, b) and (<Q_1> - <Q_2>, c), with their differences from the summer mean climatology (W/m^2). The shading denotes the values significant above 95% level of confidence using a *t*-test. The contour intervals are 100 W/m^2 in (a) and (b), and 50 W/m^2 in (c), respectively.

5 COMPARISON OF CIRCULATIONS BETWEEN ERMDR AND NON –ERMDR EPISODES

To further determine the ERMDR-related anomalous circulation characteristics, the circulations of a composite ERMDR episode are compared to those of categories C and E.

5.1 *Distribution of precipitation occurring in non–ERMDR events*

The rainfall distribution is unique at different percentiles. The pattern of averaged rainfall over the events in category C (Fig.6a) is similar, to great degree, to that of the ERMDR case, with maxima in the juncture between Anhui and Jiangxi, where the central precipitation is not less than 20 mm/d, about 40 mm/d smaller compared to that of the ERMDR event. Besides, category C-linked precipitating zones are more evenly distributed on both sides of the E-W directed Yangtze. In comparison, the pattern of category E-related means (Fig.6b) differs from the counterpart of the means across ERMDR events, with higher (lower) in the south/east (north/west) parts, and the center of maxima situated in

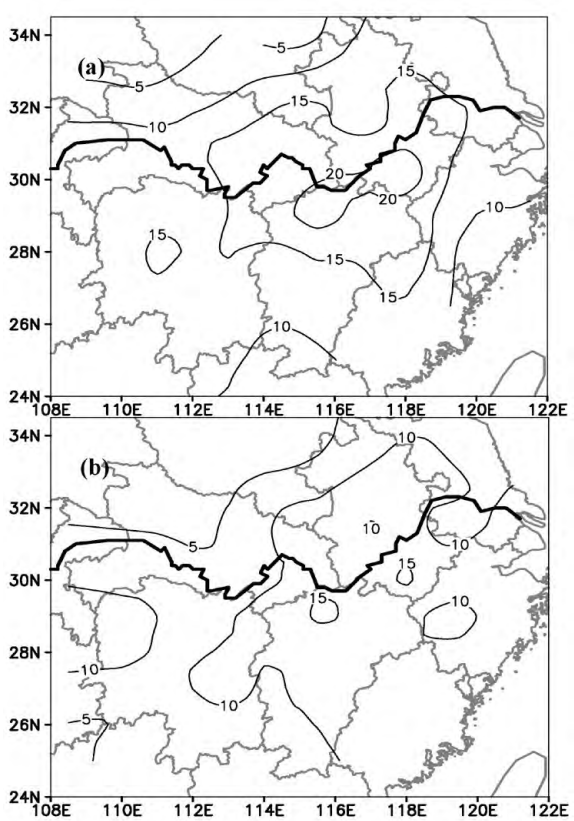

Figure 6. Patterns of mean precipitation (mm/d) over category C (a) and E (b). The thick line thereof denotes the Yangtze River.

southern Anhui and northern Jiangxi where the value is still lower at 15 mm/d in a much smaller zone.

5.2 *Anomalous circulation during non–ERMDR episodes*

Both the distribution and intensity of anomalous circulations are responsible for the changes in rainfall intensity. Category C rainfall-associated anomalies of circulation are described by means of the departures of non-divergent and divergent wind components as well as the vertical velocities. Differing from the ERMDR events, a strong departure cyclonic circulation resides in 30°-50°N, 110°-160°E at mid- and lower-levels of the troposphere, one center being in the Yangtze-Huaihe Rivers region positioned more northward and eastward than normal and another core being over the extending Kuroshio currents to the east of the Sea of Japan, centered more eastward than normal, a situation unfavorable for ERMDR event happening over the MLYV, particularly the Jiangnan region. The low latitudes west of the western Pacific are, on the whole, under the effect of an anticyclonic departure circulation. At upper levels (Fig.7c), however, the high to lower latitudes are under the impacts of anomalous circulations as a wave train of anticyclone –cyclone –anticyclone –cyclone, and the MLYV is at the middle/back of the juncture between cyclonic and anticyclonic departure circulations, differing greatly from the ERMDR-related anomaly circulations of cyclone –anticyclone at the front- and mid-MLYV (Fig.3c). From category C and ERMDR-related gradients of vorticity and stream functions and wind vectors (not shown), it is found that ERMDR-linked circulation intensity is pronouncedly strong.

As far as divergent flows are concerned, it is discovered that in the middle and lower troposphere the converging air from the SCS to the MLYV is stronger (Fig.7a, b), with the upper-air divergence over the MLYV and the oceanic waters to the east (Fig.7c). Although opposite air currents distributed at higher and low levels benefit rainfall occurrences, the diverging air is distinctly weaker in comparison to the case of ERMDR happening. Similarly, a strong rising zone (the shading of Fig.7d) is around 30°N, and the maximum exceeds 4 Pa/s, which remains much smaller than 10 Pa/s for the ERMDR episode.

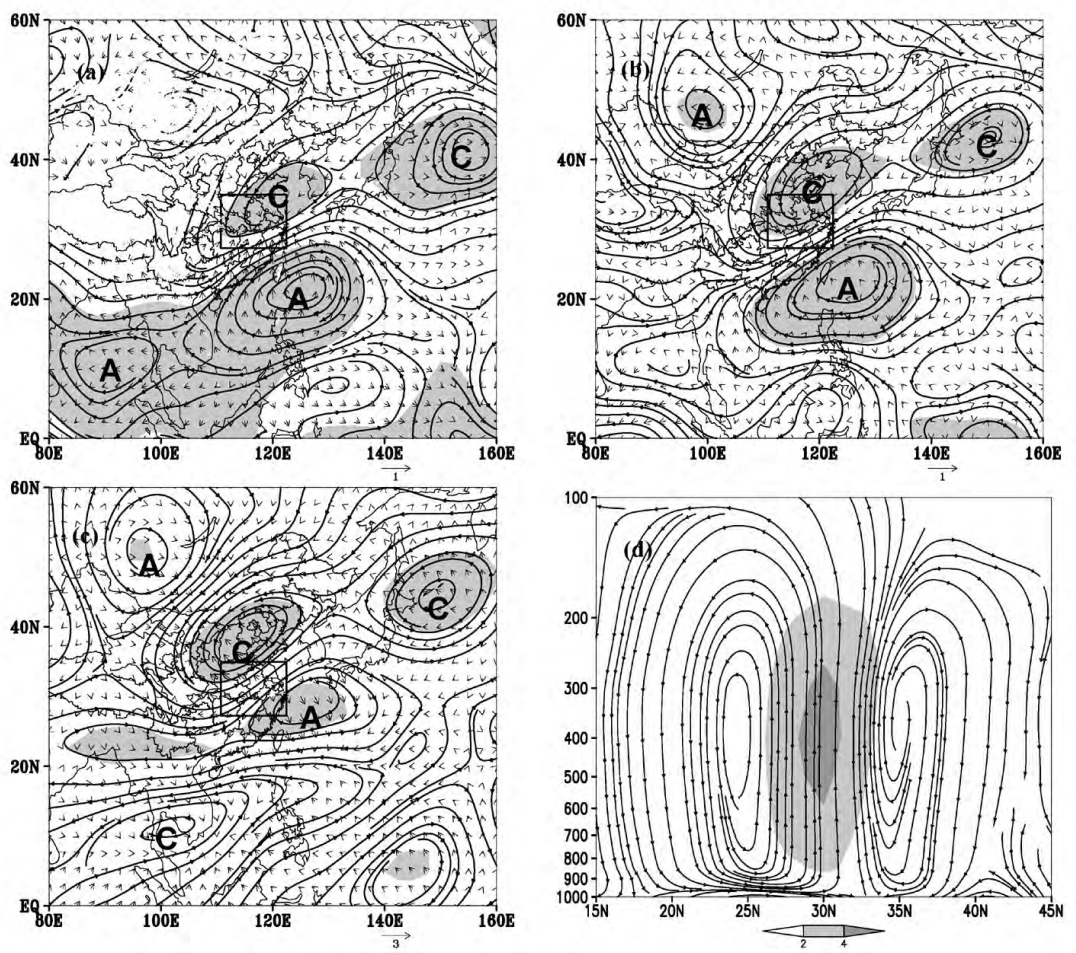

Figure 7. Anomalies of category C-related non-divergent wind (streamlines) and superimposed divergent wind (m/s) at 850 (a), 500 (b) and 200 hPa (c), as well as the cross section of anomalous zonal circulation along 110°-125°E (d). The vertical speed ω is multiplied by a factor of 100 and the shaded areas in a, b and c are statistically significant at not less than 95% level of confidence using a *t*-test.

Figure 8 presents the category E-associated circulation anomalies that are compared, separately, to those in relation to categories A and C, arriving at the following features: 1) for category C rainfall, the MLYV is under the impact of cyclonic departure circulation at middle and lower levels (Fig.8a, b, in order) and also under a convergent zone while at higher levels (Fig.8c) the valley is under the control of zonal airflows in a confluence zone of cyclonic and anticyclonic departure currents indicative of a divergent zone. The intensity of the lower-convergence/ high-level divergence is, however, much weaker in category E than in categories A and C, with insignificant vertical motion (Fig.8d); 2) on a statistical basis, composite analysis indicates that by referring to Fig.3a, b, c, Fig.7a, b, c and Fig.8a, b, c, we see that the region of category E rainfall-related circulation, significant at 95% level of confidence using a *t*-test, is very small, limited only to the MLYV. This means that, outside the valley, the circulation anomalies in other regions during the occurrence of usual rainfall episodes are not quite similar in pattern, implying that for category E rainfall events, the discrepancy in circulation anomalies is very vast between its single cases. That reveals from another perspective that the ERMDR circulation is under the joint effect of anomalous circulations over the MLYV, tropics, and mid-latitudes as well as those in the upper troposphere.

The primary patterns of water vapor transport for

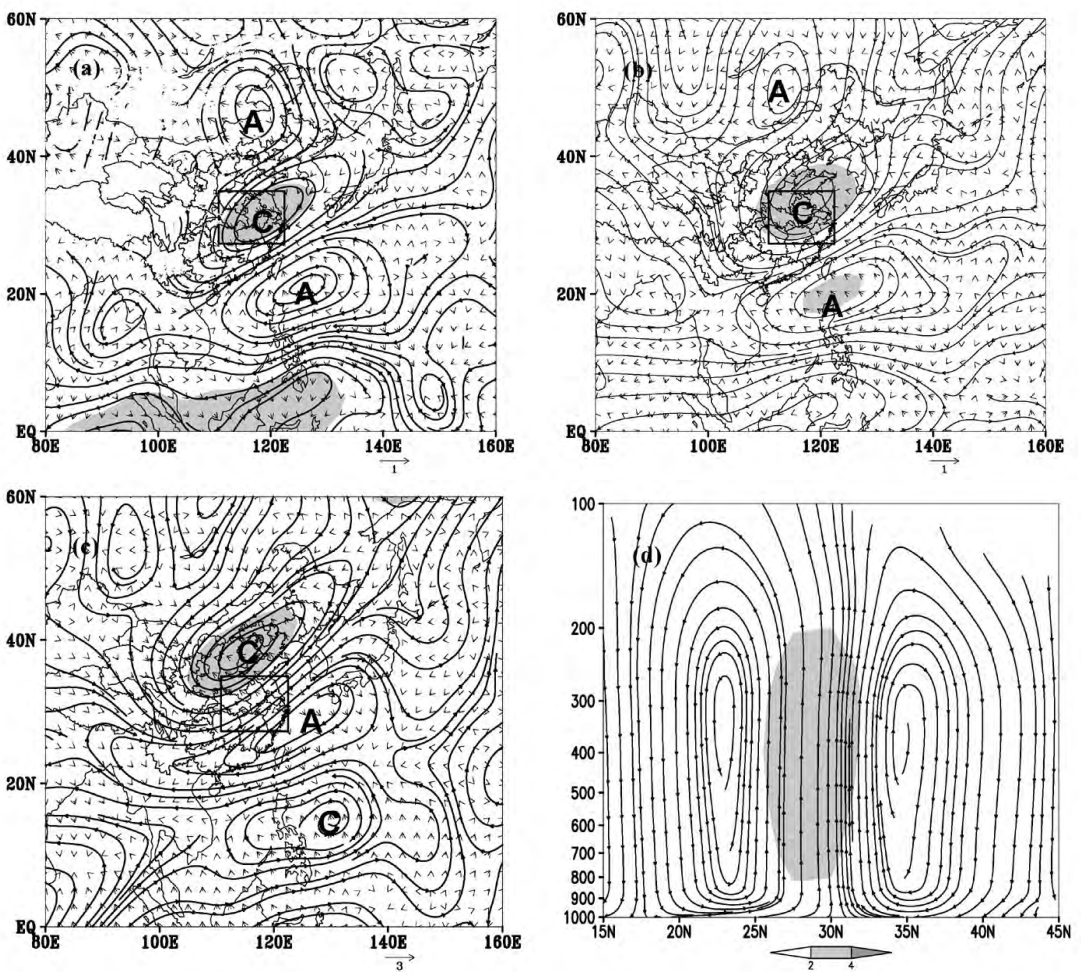

Figure 8. Same as in Fig.7 but for category E events.

different-intensity rainfall episodes are analogous except for the following: 1) When the ERMDR episode takes place, water vapor is transported both directly from the Bay of Bengal to the MLYV (denoted by streamfunctions) and out of the bay directly diverging into the valley. As categories C and E events occur (Fig.9), however, the water vapor fluxes directly diverging to the MLYV are smaller than the fluxes of water vapor from the SCS to the valley; 2) The water vapor transport in categories C and E events is considerably weaker, and the statistical significance using a *t*-test is also lower as compared to those in the ERMDR case (category A).

5.3 *Anomalies of heating related to non–ERMDR events*

The thermal forcings show some interesting features between ERMDR and non-ERMDR episodes. Firstly, the distributions of heating fields are rather similar for the rainfall episodes at these percentiles (Figs.5, 10, 11). Northwestwards from the western Pacific there

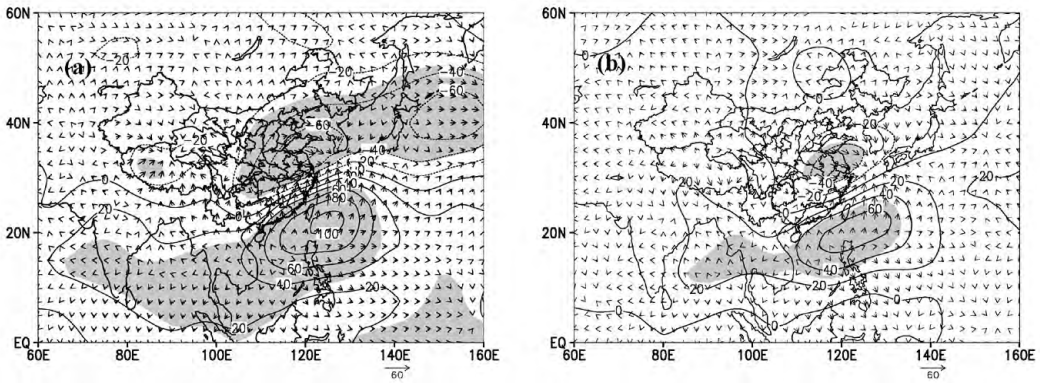

Figure 9. The streamfunctions (10^6 kg/s) of departures of vertically integrated water vapor flux related to categories C (a) and E (b) events and the corresponding divergent components (vectors, kg/ (m s)). The shading denotes the values significant at not less than 95% confidence level using a *t*-test.

are three large-valued zones, significant at the 95% level of confidence. The patterns of $<Q_1>$, $<Q_2>$ and their differences are all analogous to great degree. However, pronounced discrepancies exist in the order of magnitude between the heating fields associated with different-intensity rainfall events. In the MLYV there are positive-anomaly centers of $<Q_1>$ and $<Q_2>$ (Figs.5a, b; 10a, b; 11a, b), maximizing at 400, 150 and 100 W/m2 for the daily precipitation categories A, C and E, respectively. In contrast, oceanic waters to the south are covered with a negative-anomaly high-valued center, where there are largest values of -150 and -100 W/m^2 for the ERMDR and non-ERMDR episodes, respectively but category C (E) precipitation-shown negative-valued core is over the northwestern Pacific (SCS). In addition, over the provinces of Shaanxi, Shanxi and Ningxia north of the MLYV there resides another negative-anomaly center, with the maximum of -50 W/m^2, much smaller than the counterpart in the western Pacific. It deserves particular attention that the differences ($<Q_1>-<Q_2>$) display great discrepancies over the NW Pacific (Figs.5c, 10c, 11c). The net diabatic forcing is 3 times as strong in ERMDR as in non-ERMDR events over the western Pacific, a condition that benefits the genesis/maintenance of even more vigorous anomalous anticyclonic circulation in the NW part of the western Pacific, thereby favoring the happening of ERMDR episodes in the MLYV.

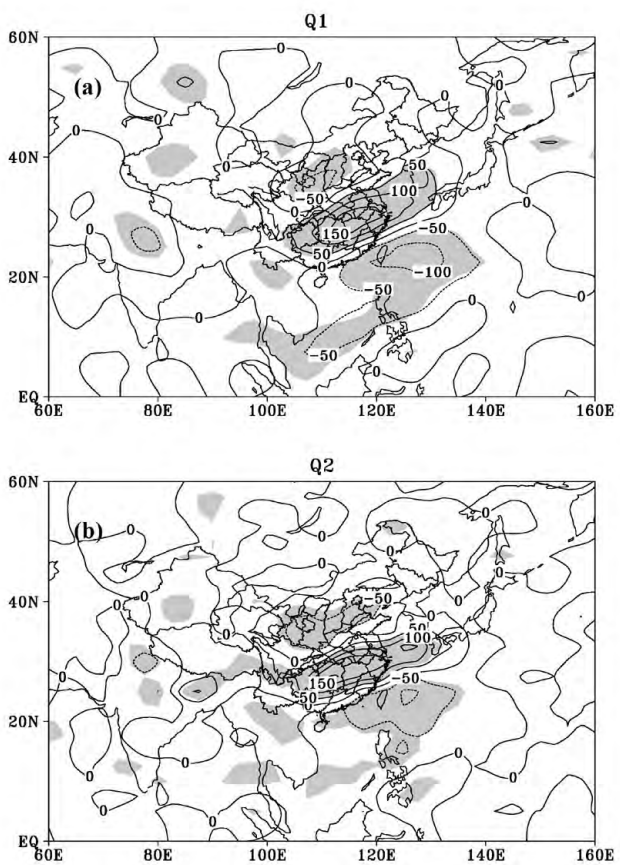

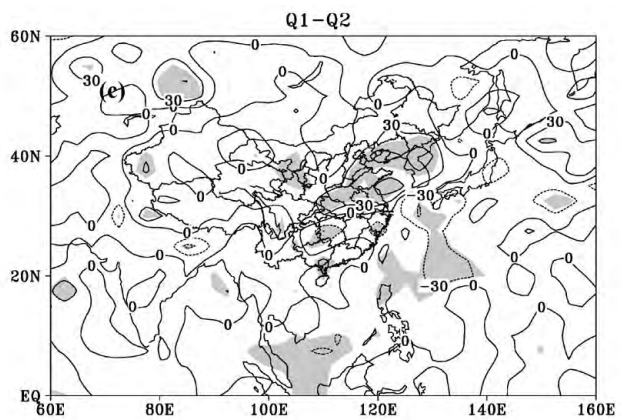

Figure 10. Vertically-integrated apparent heat source $<Q_1>$, apparent water vapor sink $<Q_2>$ and their difference ($<Q_1>-<Q_2>$) in (a), (b) and (c), in units of W/m^2, respectively, from the composite category C events. Shaded areas are above 95% level of confidence using a *t*-test. Contours are at interval of 50 W/m^2 in (a) and (b) while 30 W/m^2 in (c).

6 COMPARISON OF SSTA BETWEEN ERMDR AND NON−ERMDR EVENTS

Many studies have noted that MLYV summer precipitation is in close dependence on SSTA (Zhang et al.[8]; Wang et al.[9]; Guan and Li[10]; Xu[19]; Gong and He[36];

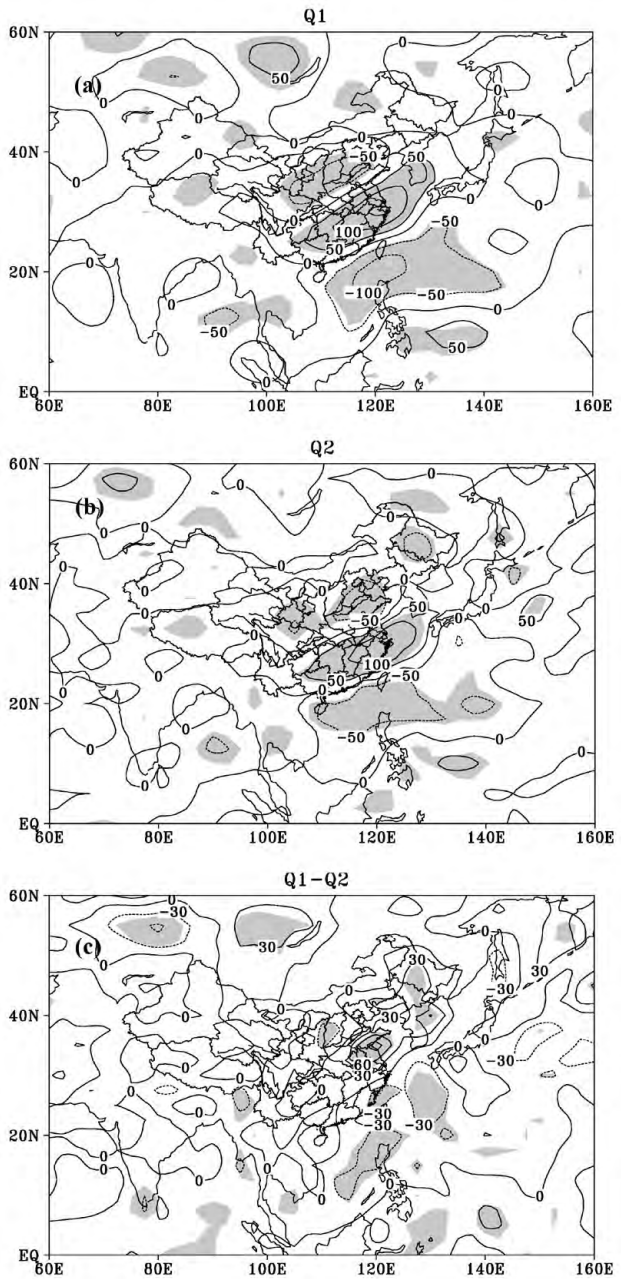

Figure 11. Same as in Fig.10 but for category E events.

Huang et al.[37]). The MLYV ERMDR formation is likely to closely relate to SSTA. Fig.12 shows the SSTA from the differences between composite JJA SST and the 1979-2008 climatology. It is clearly seen that Pacific SSTA are in a pattern of negatives (positives) in the north (south), the SSTA in the Kuroshio extension area is lower than -2℃, and strong positive SSTA cover the equatorial eastern Pacific, maximizing at >1℃, a situation that is quite similar to the SSTA pattern during a prime stage of the El Niño episode.

Compared to the SST pattern of ERMDR events (category A), the non-ERMDR category C episodes are marked by positive SSTA in the south and negative SSTA in the north, divided by the equator in the Pacific (Fig.12b), a pattern that is roughly consistent with that of ERMDR events (Fig.12a) except that the former has an intensity approximately 1/4 as big as the latter (ERMDR events), with diminished area significant at the 95% level of confidence. For the even weaker rainfall event (category E) no distinct SSTA distributed over the Pacific is found (Fig.12c), As a result, vast differences are present between SST patterns in relation to differing-strength precipitating events. This further explains that the occurrence of ERMDR episodes over the whole MLYV is likely to be closely associated with the SST pattern.

Despite the work concerning ERMDR happening remains to be conducted by means of GCMs and CGCMs, our results are of significance to understanding and predicting ERMDR episode. Non-ERMDR events, especially the weak ones thereof, do not seem to have higher statistical correlation with SSTA, implying that usual rainfall episodes bear the linkage to the evolution of atmospheric circulation by itself or other factors that are unclear hitherto.

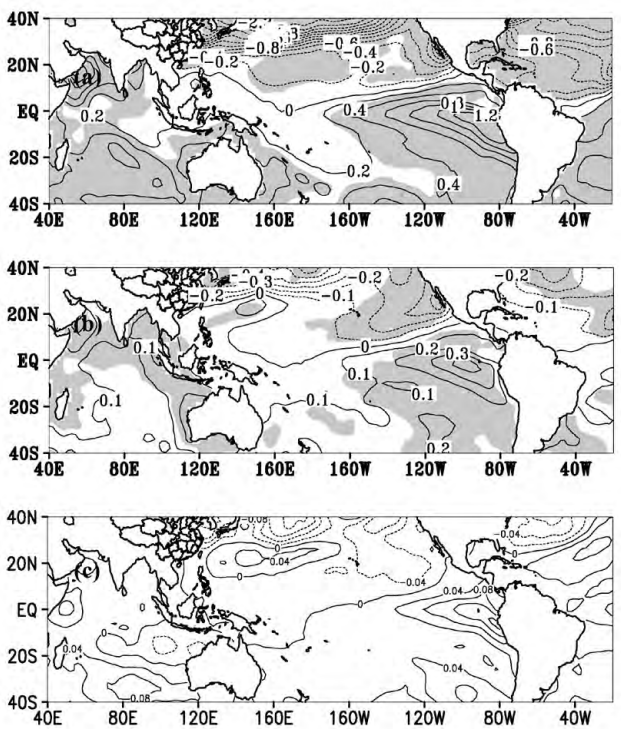

Figure 12. The distribution of differences (℃) between events-mean SST and 30-year climatology for rainfall category A (a), category C (b), and category E (c). The shading is for values above 95% level of confidence using a *t*-test.

7 CONCLUDING REMARKS

Comparison of the anomalous circulation, thermal forcings and SSTA patterns between ERMDR (category A) and non-ERMDR episodes (C, E) arrives at the following conclusions.

The threshold of ERMDR rainfall (at percentile 99) over the MLYV is 25 mm/d and its occurrences are characterized by distinct variability between years and

also between ten-day periods from June to August, with higher frequency of all categories during the Meiyu period and significantly increased ERMDR events after the 1990s.

The anomalous circulations associated with all the rainfall episodes are similar in distribution at middle and lower levels, differing greatly at higher levels. As an ERMDR event happens, the upper-air anomalous circulation is featured by an anticyclonic departure circulation over southern China that shows a more westward position than normal, a situation that is even more beneficial to the genesis of divergent air over the MLYV. Besides, the anomalous circulation is much stronger in the ERMDR than in non-ERMDR episodes.

The patterns of heating anomalies are rather similar for precipitation at all the percentiles, differing only in intensity. Towards the NW direction of the western Pacific there are three large-valued heating zones in relation to rainfall amount, which are statistically significant at not less than 95% level of confidence using a *t*-test. On the other hand, the maximal values of these centers reduce correspondingly with decreased rainfall intensity. The diabatic heating in MLYV in ERMDR events is three times as strong as that in non-ERMDR episodes and so is the strength of net diabatic heating over the western Pacific and SCS, which favors the production of an anomalous anticyclonic circulation over these oceans and on their NW side, benefiting the convergence of air and the transport of water vapor into the MLYV.

The formation of MLYV ERMDR events is likely to be associated closely with the SSTA pattern. During an ERMDR event the Pacific SSTA is in a pattern of positive in the south and negative in the northern, quite analogous to the situation in relation to the prime El Niño episode. The SSTA pattern of category C resemblances, to some degree, that of ERMDR event, just with much lower intensity at category C. However, a still weaker precipitation at category E without distinct SSTA is found. The impacts of SSTA on the happening of ERMDR events await further research.

Acknowledgement: The rainfall data used come from Nanjing Atmospheric Data Service Center in Nanjing University of Information Science & Technology. Other datasets are taken from NOAA-CIRES Climate Diagnostics Center at http://www.cdc.noaa.gov. The graphs are drawn mainly using GrADS software.

REFERENCES:

[1] MA Kai-yu, LI Bei-qun, ZENG Qing-yun. Preliminary study of large-scale flood/drought features over the Yangtze reach [J]. J Nanjing Univ (Nat Sci Ed), 1993, 29 (Spec Iss): 122-126 (in Chinese).

[2] ZHAI Pan-mao, ZHANG Xue-bin, WAN Hui, et al. Trends in total precipitation and frequency of daily precipitation extremes over China [J]. J Climate, 2005, 18(7): 1 096-1 108.

[3] BAI Ai-juan, LIU Xiao-dong. Characteristics of rainfall variation over east china for the last 50 years and their relationship with droughts and floods [J]. J Trop Meteorol, 2010, 16(3): 255-262.

[4] GUAN Zhao-yong, LIN Chun-yu. On the circulation characteristics at mid and lower latitudes of the eastern hemisphere during the years of anomalous Meiyu rainfall [J]. Sci Meteorol Sinica, 1989, 9(1): 80-85 (in Chinese).

[5] WANG Li-juan, CHEN Xuan, GUAN Zhao-yong et al. Relationships between the position variation of the west Pacific subtropical high and the diabatic heating during persistent intense rain events in Yangtze-Huaihe Rivers basin [J]. J Trop Meteorol, 2012, 18(4): 528-536.

[6] LI Li-ping, WANG Chao, ZHANG Kai-mei. Possible relationship between the interannual anomaly of the tropical Pacific sea surface height and summer precipitation in China [J]. J Trop Meteorol, 2013, 19(1): 16-2.

[7] TAO Shi-yan, LI Ji-sun, WANG Ang-sheng. Eastern Asian monsoon in relation to floods/droughts over China [J]. Disas Reduct China, 1997, 7(4): 17-24 (in Chinese).

[8] ZHANG Ren-he, SUMI Akimasa, KIMOTO Masahide. A diagnostic study of the impact of El Niño on the precipitation in China [J]. Adv Atmos Sci, 1999, 16(2): 229-241.

[9] WANG Bin, YANG Jing, ZHOU Tian-jun. In terdecadal changes in the major modes of Asian-Australian monsoon variability: Strengthening relationship with ENSO since the late 1970s [J]. J Climate, 2008, 21(8): 1 771-1 789.

[10] GUAN Zhao-yong, LI Li-ping. Interannual variability of summer climate of China in association with ENSO and the Indian Ocean Dipole [M]// Regional Climate Studies of China. Spring-Verlag Berlin Heidelberg, 2008: 120-147.

[11] SAJI N H, YAMAGATA T. Possible impacts of the Indian Ocean Dipole mode events on global climate [J]. Climate Res, 2003, 25(2): 151-169.

[12] YANG Xia, GUAN Zhao-yong, ZHU Bao-lin. Role of Indian Ocean dipole events in the influence of ENSO on the summer rainfall and temperature in China [J]. J Nanjing Inst Meteorol, 2007, 30(2): 170-177 (in Chinese).

[13] WANG Zun-ya, DING Yi-hui. Climate features of intraseasonal oscillations of summer rainfall over the mid-lower reaches of Yangtze River in the flood and drought years [J]. J Appl Meteor Sci, 2008, 19 (6): 710-715 (in Chinese).

[14] TAO Shi-yan, ZHANG Qing-yun, ZHANG Shun-li. The great floods in the Changjiang river valley in 1998 [J]. Clim Environ Res, 1998, 3(4): 290-299 (in Chinese).

[15] ZHI Xie-fei, ZHANG Ling, PAN Jia-lu. An analysis of the winter extreme precipitation events on the background of climate warming in southern China [J]. J Trop Meteorol, 2010, 16(4): 325-332.

[16] ZHANG Shun-li, TAO Shi-yan. The influences of Tibetan plateau on weather anomalies over Changjiang river in 1998 [J]. Acta Meteorol Sinica, 2002, 60(4): 442-452 (in Chinese).

[17] WU Zhi-wei, HE Jin-hai, HAN Gui-rong, et al. The relationship between MeiyYu in the mid-and-lower reaches of the Yangtze River valley and the boreal spring southern hemisphere annual mode [J]. J Trop Meteorol, 2006, 12(1): 89-90.

[18] MAO Jiang-yu, WU Guo-xiong. Intraseasonal variability in the Yangtze-Huaihe river rainfall and subtropical high during the 1991 Meiyu period [J]. Acta Meteorol Sinica,

2005, 63(5): 162-170 (in Chinese).
[19] XU Hai-ming. Effects of eastern Atlantic SSTA on flood over Jiang-huai valleys in summer of 1991 [J]. J Nanjing Inst Meteor, 1996, 19(3): 329-334 (in Chinese).
[20] MEI Shi-long, GUAN Zhao-yong. Activities of baroclinic wave packets in the upper troposphere related to Meiyu of 2003 in the Yangtze River-Huaihe River valley [J]. Chin J Atmos Sci, 2008, 32 (6): 1 333-1 340 (in Chinese).
[21] MEI Shi-long, GUAN Zhao-yong. Propagation of baroclinic wave packets in upper troposphere during the Meiyu period of 1998 over middle and lower reaches of Yangtze River valley [J]. J Trop Meteorol, 2009, 25(3): 300-306 (in Chinese).
[22] WANG Li-juan, GUAN Zhao-yong, HE Jin-hai. The circulation background of the extremely heavy rain causing severe floods in Huai River vally in 2003 and its relationships to the apparent heating [J]. Sci Meteorol Sinica, 2008, 28(1): 1-7 (in Chinese).
[23] ZHOU Yu-shu, GAO Shou-Ting, DENG Guo. A diagnostic study of water vapor transport and budget during heavy precipitation over the Changjiang River and the Huaihe River basins in 2003 [J]. Chin J Atmos Sci, 2005, 29(2): 195-204 (in Chinese).
[24] KUNKEL K E, ANDSAGER K, EASTER LING D R. Long-term trends in extreme precipitation events over the conterminous United States and Canada [J]. J Climate, 1999, 8(2): 2 515-2 527.
[25] YAMAMOTO R, SAKURAI Y. Long-term intensification of extremely heavy rainfall intensity in recent 100 years [J]. World Resource Rev, 1999, 11(2): 271-282.
[26] QIAN Wei-hong, LIN Xiang. Regional trends in recent precipitation indices in China [J]. Meteorol Atmos Phys, 2005, 3(4): 193-207.
[27] E. KALNAY, M. KANAMITSU, R. KISTLER et al. The NCEP/NCAR 40-year reanalysis project [J]. Bull Amer Meteorol Soc, 1996, 77(3): 437-471.
[28] JONES P D, RAPER S C B, BRADLEY R S, et al. Northern hemisphere surface air temperature variations: 1851-1984 [J]. J Clim Applied Meteorol, 1986, 25 (2): 161-171.
[29] LUO Hui-bang, YANAI Michio. The large-scale circulation and heat sources over the Tibetan Plateau and surrounding areas during the early summer of 1979. Part II: Heat and moist budgets [J]. Mon Wea Rev, 1984, 112(5): 966-989.
[30] SU Bu-da, JIANG Tong, REN Guo-yu, CHEN Zheng-hong. Observed Trends of Precipitation Extremes in the Yangtze River Basin during 1960 to 2004 [J]. Adv Clim Change Res, 2006, 2(1): 9-14 (in Chinese).
[31] TAO Shi-yan, XU Shu-ying. Some aspects of the circulation during the periods of the persistent drought and flood in Yantze and Hwai-ho valleys in summer [J]. Acta Meteorol Sinica, 1962, 32(1): 1-32 (in Chinese).
[32] CHEN Yi-min, QIAN Yong-fu. The analysis and numerical simulation of atmospheric circulation of Mei-yu rainfall in the mid-lower reaches of the Changjiang River [J]. J Trop Meteorol, 2006, 22(1): 26-33 (in Chinese).
[33] MURAKAMI T. The general circulation and water-vapor balance over the Far East during the rainy season [J]. Geophys Mag, 1959, 29(2): 137-171.
[34] DING Yi-hui. Summer monsoon rainfalls in China [J]. J Meteorol Soc Jpn, 1992, 70(1): 373-396.
[35] GILL A E. Some simple solutions for heat-induced tropical circulation [J]. Quart J Met Soc, 1980, 106 (5): 447-462.
[36] GONG Zhen-song, HE Min. Relationship between summer rainfall in Changjiang river valley and SSTA of various seasons [J]. Meteorol Mon, 2006, 32 (1): 51-62 (in Chinese).
[37] HUANG Mao-dong, LIAO Shi-xiang, ZHANG Chen-hui. Analysis of the mechanism of Pacific SSTA influencing extreme rainfall precipitation events in annually first raining season in Guangdong [J]. J Trop Meteorol, 2009, 25 (4): 413-420 (in Chinese).

Citation: HAN Jie, GUAN Zhao-yong and LI Ming-gang. Comparisons of circulation anomalies between the daily precipitation extreme and non-extreme events in the middle and lower reaches of Yangtze River in boreal summer [J]. J Trop Meteorol, 2015, 21 (2): 131-142.